Macromolecular Chemistry and Physic
www.mcp-journal.d

Dot Nanopattern Self-Assembled from Rod-Coil Block Copolymer on Substrate

Bo Sun, Zhanwen Xu, Zhengmin Tang, Chunhua Cai, and Jiaping Lin**

Nanoscale dot patterns are important in various fields. However, it is still a challenge to fabricate ordered nanopatterns on substrates through a polymer self-assembly approach. In this work, it is reported that polypeptide-based rod-coil block copolymers can self-assemble into surface micelles on substrates, thus forming dot nanopatterns. The size of the surface micelles is readily adjusted by the degree of the polymerization of the block copolymers. It is found that most of the surface micelles are in a sixfold coordinated lattice, indicating an ordered array feature. Defects such as fivefold coordination arrays and sevenfold coordination arrays are also observed, which are derived from the nonuniform size of the micelles and the existence of nonspherical micelles. The experimental findings are well modelled by dissipative particle dynamics theoretical simulations, and the simulations provide more detailed information, such as the packing manner of the polymer chain in the surface micelles.

1. Introduction

Ordered surface nanostructures at the nanometer scale endow the materials with unique and intriguing properties, which have attracted increasing attention in recent years.[1–6] A number of efforts have been devoted to constructing well-ordered surface nanostructures on substrates, such as thermal/solvent-vapor annealing,[7,8] lithography,[9] and a breath figure (BF) method.[10,11] However, these approaches usually suffer from multistep procedures or have high processing costs. For example, the solvent-vapor annealing method often requires complex equipment, and the procedures are time consuming. The self-assembly of block copolymers generates diverse nanostructures,[12–15] which may be a facile way to produce surface nanostructures on substrates without expensive devices or complex processes.[16,17] However, in the limited examples regarding the self-assembly of block copolymers at a selective solvent/substrate interface (interface self-assembly of block copolymer in solution), such as homogeneous films or irregular surface nanostructures are usually produced.[18,19] Thus, it is still a challenge to prepare ordered surface nanostructures on a substrate through a block copolymer self-assembly approach.

Among the surface nanostructures, dot nanopatterns have attracted considerable interest because of their applications in a variety of nanodevices, such as optical devices[20] and DNA or protein electrophoresis.[21] To optimize the properties of nanodevices, it is essential to control the size and arrangement of each dot. Thus, for an ordered surface nanostructure, the ordering feature, defined as the array characteristics of the nanostructure, is an important aspect that should be discussed.[22,23] Theoretical model studies have well explored the arrangement characteristics of surface nanostructures; however, in experiments little is known about the arrangement characteristics of surface nanostructures on substrates.

Herein, we report that poly(γ-benzyl-L-glutamate)-*block*-poly(ethylene glycol) (PBLG-*b*-PEG) rod-coil block copolymers can self-assemble into dot nanopatterns on a polystyrene (PS) substrate. The size of the dot-like surface micelles is readily regulated by the degree of polymerization of the block copolymers. In the patterns, most of the surface micelles are in a sixfold coordinated lattice. Theoretical simulations qualitatively reproduce the experiments and provide polymer packing information of the surface micelles. This research provides guidance for the interfacial assembly of rod-coil block copolymers and provides a facile and effective method for the preparation of materials with surface structures.

2. Results and Discussion

The self-assembly preparation process is shown in **Scheme 1**. The PS substrate was prepared by spin-coating PS solutions on a Si wafer. After heat treatment and extensive rinsing with toluene, a thin PS film was irreversibly adsorbed on the substrate, which is stable in organic solvents.[24,25] PBLG-*b*-PEG is a typical rod-coil block copolymer in which the PBLG adopts an α-helix conformation that acts as a rigid rod, and PEG is a typical flexible polymer. The self-assembly process involves two steps (Scheme 1). In the first step, the substrate was immersed

B. Sun, Dr. Z. Xu, Z. Tang, Prof. C. Cai, Prof. J. Lin
Shanghai Key Laboratory of Advanced Polymeric Materials
Key Laboratory for Ultrafine Materials of Ministry of Education
Frontiers Science Center for Materiobiology and Dynamic Chemistry
School of Materials Science and Engineering
East China University of Science and Technology
Shanghai 200237, China
E-mail: caichunhua@ecust.edu.cn; jlin@ecust.edu.cn

The ORCID identification number(s) for the author(s) of this article can be found under https://doi.org/10.1002/macp.202000254.

DOI: 10.1002/macp.202000254

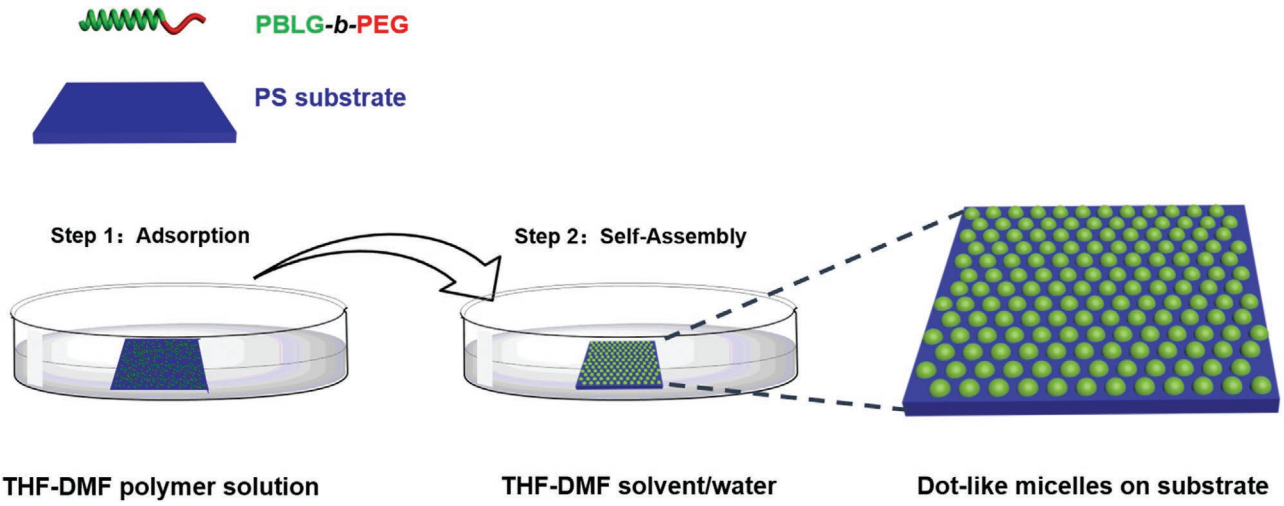

Scheme 1. Scheme of the self-assembly of the PBLG-*b*-PEG rod-coil block copolymers into surface micelles on a PS substrate.

into the solution of PBLG-*b*-PEG in tetrahydrofuran/*N*,*N*′-dimethylformamide mixture (THF/DMF, 3/7 v/v) with the PS facing up. In the second step, the substrate was transferred into a fresh THF/DMF solvent (3/7 v/v), and selective solvent (water) was added gradually.

We first monitored the morphology of the substrate under various conditions to explore the formation process of the surface nanopattern (**Figure 1**). As shown in Figure 1a, the atomic force microscopy (AFM) image reveals that the surface of the blank substrate is smooth. In the first step, for a representive sample $PBLG_{133}$-*b*-PEG_{113} (the subscripts denote the degree of polymerization, DP, for each block), after 1 h of adsorption, a rough surface is observed on the substrate, which indicates the adsorption of the block copolymers on the substrate (Figure 1b). By comparing the surface morphology at different adsorption times, it is deduced that after 1 h, the adsorption process of the block copolymers reaches a saturated state (Figure S3, Supporting Information). In the second step, as shown in

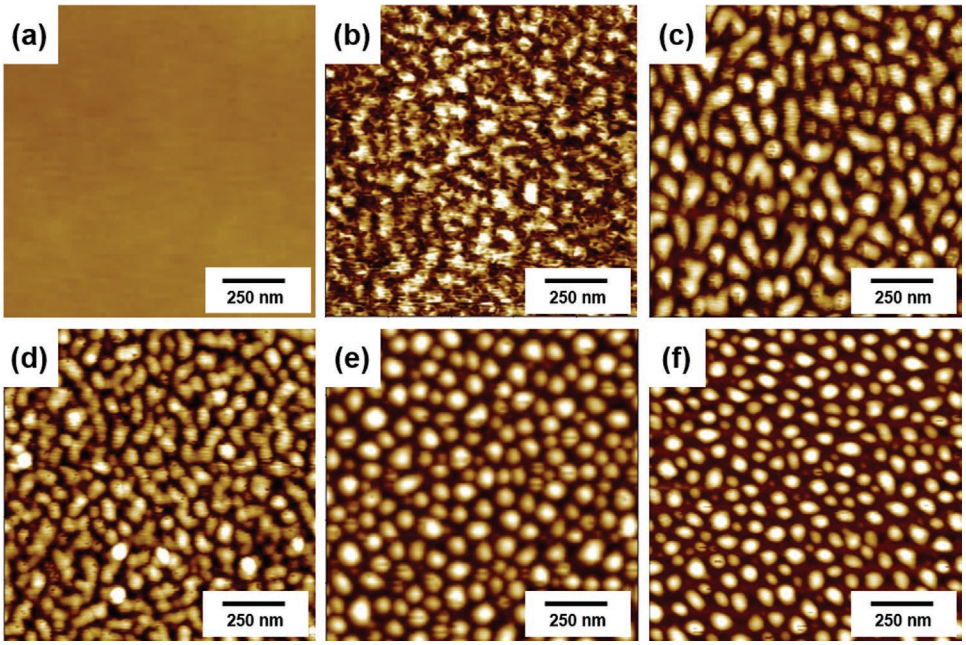

Figure 1. AFM observation of the formation process of dot-like structures by the $PBLG_{133}$-*b*-PEG_{113} block copolymers. a) PS substrate. b) Step 1: substrate adsorbed by the block copolymers without adding water. Step 2: formation process of the surface micelles as a function of the added water content: c) 4.8, d) 13.0, e) 23.1, and f) 28.6 vol%. The initial solvent was THF/DMF = 3/7 v/v. No water washing was performed before the AFM observation in panels (b)–(e), and the sample in panel (f) was washed with water before the AFM observation. The initial concentration of the block copolymer is 0.2 g L^{-1}, and the experiment temperature is 20 °C.

Figure 1c, when 4.8 vol% (the volume percentage of the added water relative to the whole solution volume) water is added, the block copolymers form irregular assemblies on the substrate. When the water content is 13.0 vol%, these irregular assemblies become smaller (Figure 1d). When the water content increases to 23.1 vol%, as shown in Figure 1e, dot nanopatterns are formed. Finally, when the water content is further increased, no significant change in the morphology of the dot nanopatterns is observed. Figure 1f shows the morphology of the nanopatterns formed at a water content of 28.6 vol%. As can be seen, a well-defined dot nanopattern is obtained.

By studying the formation process of the surface micelles, an adsorption-assembly process is suggested, which includes the PBLG-*b*-PEG block copolymers adsorbing on the substrate and the adsorbed block copolymers self-assembling into surface micelles subsequently. There are strong attractions between the PBLG and PS segments, including hydrophobic and π–π interactions,[26–29] which drive the adsorption of PBLG-*b*-PEG block copolymers on the PS substrate. Since the PBLG blocks are rigid (the persistence length of PBLG is up to 200 nm[30]) and from the theoretical and experimental studies of adsorption behavior of block copolymers on interfaces,[31–33] we can deduce that the PBLG-*b*-PEG block copolymers could lie down on the substrate to form a thin film.[32] With the addition of water in the second step, because of the hydrophobicity of the PBLG and PS segments, the PBLG segments tend to form a core on the PS substrate, while the hydrophilic PEG segments form a shell wrapping the core to lower the contact of water to both the PS substrate and the PBLG. The morphology of the assembly changes with the water content. At a water content of 23.1 vol%, regular surface micelles are formed. When further increasing the water content, there is no evident change in the morphology of the surface micelles since the mobility of the block copolymer segment is frozen. These surface micelles arrange into an ordered dot nanopattern on the substrate.

It is worth noting that the rod nature of the PBLG blocks is essential to form such surface micelles. Since PS is a flexible polymer and the interaction between PBLG/PS pairs is comparable to that between PS/PS pairs,[30,34] we replaced the PBLG-*b*-PEG rod-coil block copolymers with PS-*b*-PEG coil–coil block copolymers to assemble on the PS substrate under similar conditions. It was found that PS-*b*-PEG can also assemble on the surface of the substrate. However, instead of ordered surface micelles, a rough surface with an irregular pattern on the substrate is formed by the PS-*b*-PEG block copolymers (Figure S5, Supporting Information). These results indicate that the rigid nature of the PBLG segments is important to create ordered nanopatterns.

The typical morphologies of the surface micelles were characterized by AFM analyses (**Figure 2**). Figure 2a-c shows that the substrates are fully covered by surface micelles after self-assembling with $PBLG_{91}$-*b*-PEG_{113}, $PBLG_{133}$-*b*-PEG_{113}, and $PBLG_{180}$-*b*-PEG_{113} block copolymers. The size of the micelles increases with the DP of the PBLG blocks. The enlarged AFM image clearly reveals the dot-like morphology of the surface micelles formed by the $PBLG_{133}$-*b*-PEG_{113} block copolymers (Figure 2d). From the corresponding height profile (Figure 2e), an average diameter and height of ≈74 and 16 nm, respectively,

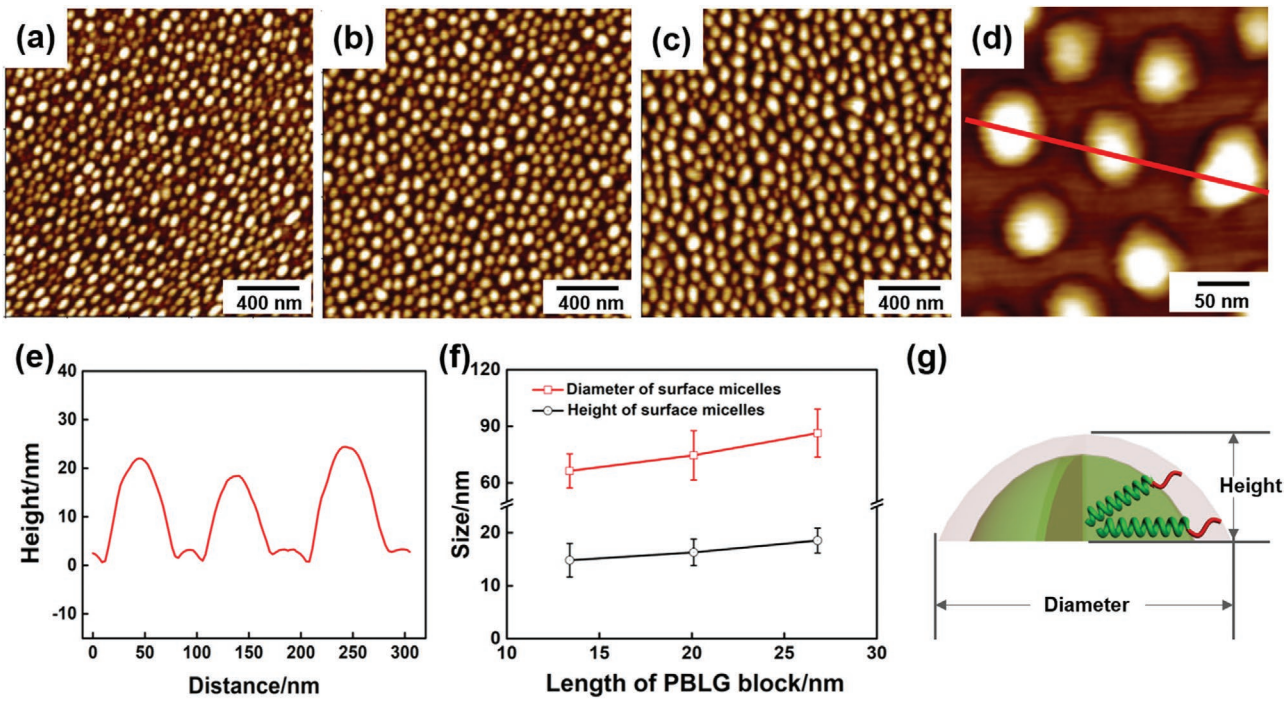

Figure 2. Morphology and structure of the surface micelles. AFM images of the dot surface nanostructures self-assembled from a) $PBLG_{91}$-*b*-PEG_{113}, b) $PBLG_{133}$-*b*-PEG_{113}, and c) $PBLG_{180}$-*b*-PEG_{113}. d) Enlarged view of the surface micelles formed by $PBLG_{133}$-*b*-PEG_{113}. e) Height profile of the surface micelles along the red line shown in (d). f) Plots of the length of the PBLG block versus the diameter and height of the surface micelles. g) Scheme of the structure of the surface micelles.

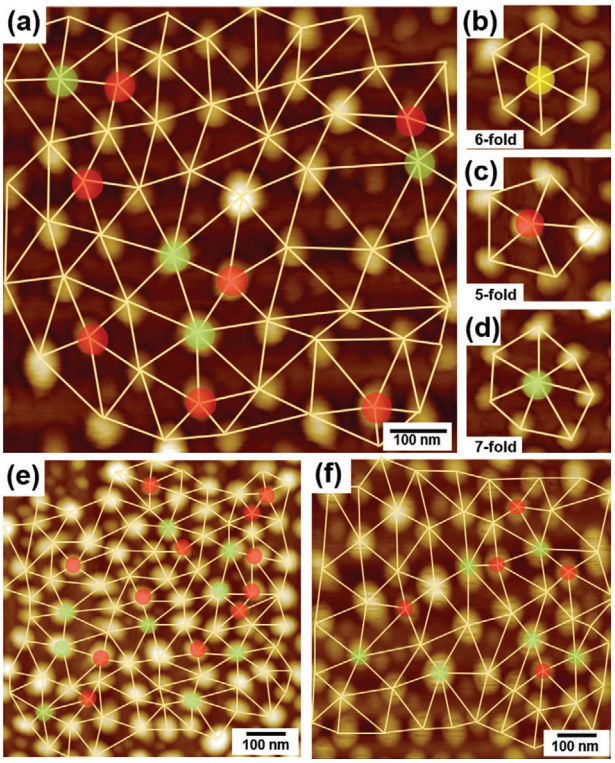

Figure 3. Array feature analysis of the surface micelles formed by the PBLG-*b*-PEG block copolymers with various DP values of the PBLG blocks. a) DP = 133; b–d) Enlarged views of the sixfold, fivefold, and sevenfold coordinated surface micelles, respectively. e) DP = 91. f) DP = 180. The red and green dots represent the fivefold coordinated micelles and sevenfold coordinated micelles, respectively.

are obtained for the $PBLG_{133}$-*b*-PEG_{113} surface micelles. A static analysis reveals that as the DP of the PBLG blocks increases, the average diameter of micelles increases in an approximately linear fashion (Figure 2f); that is, from ≈66 nm (DP of the PBLG block is 91) to ≈74 nm (DP of the PBLG block is 133) and then to ≈83 nm (DP of the PBLG block is 180). Meanwhile, the height of the surface micelles slightly increases from ≈14 to 18 nm.

Since these surface micelles are composed of a PBLG core and PEG shell, by analyzing the relationship between the diameter of the surface micelles and the length of the block copolymers, the packing manner of the PBLG-*b*-PEG block copolymers in the surface micelles can be deduced. The length of PBLG rigid segments can be estimated from their DP.[26] The lengths of the PBLG blocks with DP = 91, 133, and 180 are ≈13.7, 20.1, and 27.1 nm, respectively. From the diameter of the surface micelles and the length of the PBLG blocks, we speculate that the PBLG rigid blocks arrange in a head-to-head mode in the core of the surface micelles, and the PEG blocks extend into the water. In such a packing manner, taking the micelles from the $PBLG_{133}$-*b*-PEG_{113} block copolymers as an example, the core region formed by the PBLG blocks is ≈40.2 nm, and the shell occupied by the PEG blocks is ≈16.9 nm, which accounts for a reasonable stretching degree of 43% (the full stretched length of PEG_{113} is ≈39 nm).[35,36] **Figure 3**g illustrates the structure of the surface micelles self-assembled from the PBLG-*b*-PEG block copolymers on the PS substrate.

For an ordered dot surface nanopattern, the dot array characteristics are an essential aspect that should be discussed.[37,38] For spherical particles on a flat substrate, it is well known that the ideal packing mode is a sixfold coordinated lattice, i.e., the particles take the form of domain with six nearest neighbors.[39] However, in practice, due to the imperfect shape of spherical particles, the patterns usually contain other array modes, typically fivefold coordinated lattices that are characterized by +1 disclinations and sevenfold coordinated lattices that are characterized by –1 disclinations.[40–42] In this work, the array features of the surface micelles are determined by Delaunay triangulation, which can analyze the lattice by identifying the nearest neighbors of each particle.[43] Once the position of the particle is determined, the coordination number can be obtained by counting the nearest neighbors of each particle. As shown in Figure 3a, for the nanopattern formed by the $PBLG_{133}$-*b*-PEG_{113} block copolymers, the observed array types include sixfold coordination, fivefold coordination, and sevenfold coordination. The enlarged images for these array types are shown in Figure 3b-d. Similarly, these array types are also observed for the nanopatterns formed by the $PBLG_{91}$-*b*-PEG_{113} block copolymers (Figure 3e) and $PBLG_{180}$-*b*-PEG_{113} block copolymers (Figure 3f).

We then analyzed the number and array features of the surface micelles to acquire accurate arrangement characteristics. The average numbers of surface micelles per square micrometer (μm^2) assembled by $PBLG_{91}$-*b*-PEG_{113}, $PBLG_{133}$-*b*-PEG_{113}, and $PBLG_{180}$-*b*-PEG_{113} are 119, 98, and 58, respectively. The array feature analysis reveals that the sixfold coordination array is the dominant type for the surface micelles in all systems, and the fivefold coordination and the sevenfold coordination arrays are the minority. **Table 1** summarizes the array features of the surface micelles formed by various PBLG-*b*-PEG block copolymers. The micelles with sixfold coordination account for

Table 1. Array features of the surface micelles formed by the PBLG-*b*-PEG block copolymer with various DP of the PBLG block.

DP of PBLG	Number of surface micelles on substrate[a)]	Sixfold coordinated surface micelles		Fivefold coordinated surface micelles (+1 disclination)		Sevenfold coordinated surface micelles (–1 disclination)	
		Number	%	Number	%	Number	%
91	1192	697	58.5	268	22.5	227	19.0
133	981	623	63.5	201	20.5	157	16.0
180	583	384	65.9	105	18.0	94	16.1

[a)]The number of surface micelles was counted from 10 images of the sample (each image has a size of 1 × 1 μm).

58–66% of the total surface micelles. The surface micelles with fivefold coordination account for 18–22%, and those with sevenfold coordination account for 16–19%.

Theoretically, the ideal packing mode of spherical particles on a flat substrate is a sixfold coordinated lattice, and the fivefold and sevenfold coordinated lattices are called defects. We then analyzed the origin of the defects in the present system. For the present system, from the morphology and size characteristics of these surface micelles, we infer that the fivefold and sevenfold coordination arrays are mainly generated from the nonuniform size of the micelles. We analyzed the size of the surface micelles by randomly collecting 500 surface micelles self-assembled from each of the three block copolymers. As shown in **Figure 4**, these surface micelles are not uniform but are distributed in size. The nonuniform size of the micelles may result from both the dispersity nature in chain length of the PBLG-*b*-PEG block copolymers and the nonuniform aggregation number of each surface micelle.[44,45] In addition, the size distribution of the micelles is not symmetric. The asymmetry of micelle distribution can be described by skewness, which is a measure of the distortion of the probability distribution.[46] The analysis reveals that in all systems, the distribution of the micelles displays positive skewness, which means that more than 50% of the surface micelles are smaller than the average size. This can explain why there are more surface micelles observed with a fivefold coordination than those observed with a sevenfold coordination. As compared to the micelles with a sixfold coordination, the micelles with a fivefold coordination are usually smaller in size while the micelles with a sevenfold coordination are usually have a larger size.[47]

In addition to the nonuniform size of the micelles, the presence of micelles with a nonspherical shape should also cause array defects.[48] As seen from Figures 2 and 3, some of the surface micelles are not in a well-defined spherical shape but in an ellipsoidal shape. The nonspherical surface micelles disturb the ideal packing mode of the spherical surface micelles (sixfold coordinated lattices); as a result, array defects, including the fivefold and sevenfold coordinated lattices, are induced.

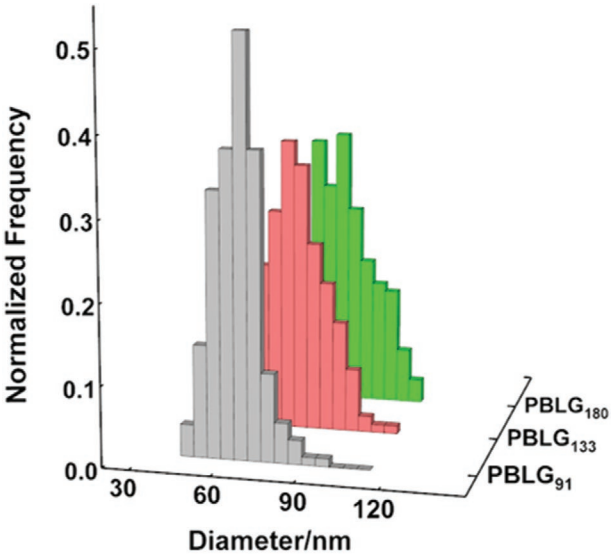

Figure 4. Size distribution diagram of the surface micelles assembled by block copolymers with various DP values of the PBLG block.

To support the experimental results, a coarse-grained DPD simulation[49,50] was used to study the nanostructures and array characteristics of the surface micelles. In the DPD methods, the PBLG-*b*-PEG block copolymers are coarse-grained into RC copolymer chains, where the R and C beads represent the PBLG and PEG blocks, respectively. **Figure 5**a shows the R_6C_5 model block copolymer corresponding to $PBLG_{133}$-*b*-PEG_{113}.

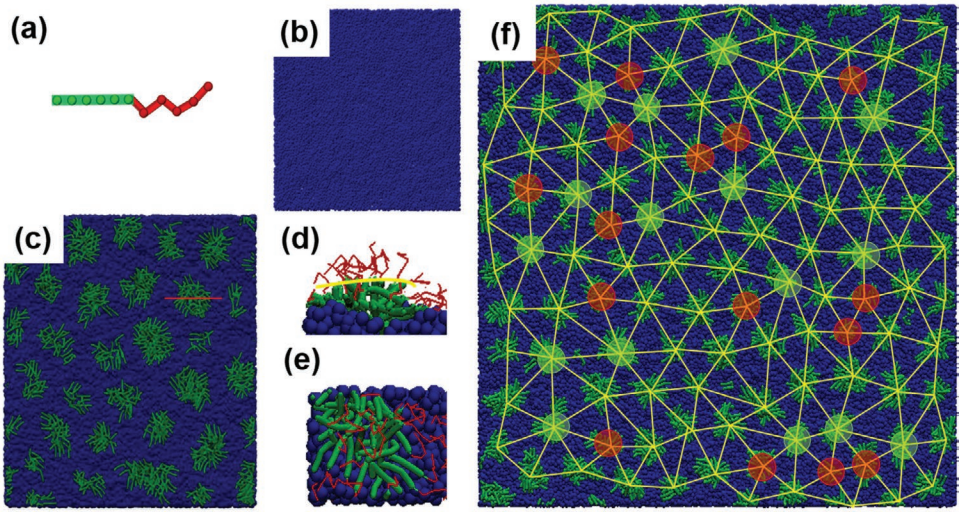

Figure 5. Simulation insight into the structure and array features of the surface micelles. a) DPD model of the R_6C_5 rod-coil block copolymers. The rod and coil blocks are colored green and red, respectively. b) DPD model of the PS substrate (colored in blue). c) A simulation prediction of a substrate on which surface micelles are formed by the rod-coil block copolymers. d) Cross-sectional images of the surface micelles along the red line in (c). e) Cross-sectional images of the surface micelles along the yellow line in (d). f) Array feature analysis of the surface micelles formed by R_6C_5. The red and green dots represent the micelles that were arranged in fivefold coordination array and sevenfold coordination array, respectively.

The substrate covered by a PS layer was coarse-grained into a planar substrate (W) covered by homopolymers (P), as shown in Figure 5b. The selective solvents are denoted by S beads. The interaction parameters between the *i*- and *j*-component beads are represented by the parameter a_{ij}. The interaction parameter between the hydrophobic rod blocks and the solvent (a_{RS}) is set as 120 to correspond with the experiments. Simultaneously, to guarantee that the RC block copolymers can adsorb on the substrate, the interaction parameter between the R blocks and homopolymer (a_{RP}) is set as 25. Then, after the system in the simulations reaches a steady state, the self-assembled nanostructures are collected. Section S10 of the Supporting Information provides more details about the DPD simulation methods and the parameter settings.

We first examined the self-assembly of R_6C_5 on the substrate, which corresponds to the self-assembly of the $PBLG_{133}$-*b*-PEG_{113} block copolymer. As shown in Figure 5c, the theoretical simulation shows that R_6C_5 block copolymers self-assemble into surface micelles on the substrate. The cross-sectional image reveals that R blocks form the core adhering on the substrate and C blocks form the shell (Figure 5d). Furthermore, the packing mode of the block copolymers in the surface micelles can be observed in the cross-sectional image. As seen from Figure 5e, the rigid R segments arrange in a head-to-head manner in the core of the micelle, and the flexible C segments in the micelle shell extend to the solution. The block copolymer packing mode in the surface micelles proposed from the experimental characterizations is well supported by this theoretical simulation result. Then, we varied the number of beads in the R blocks from 5 to 7 (the number of C beads remained at 5) to study the effect of DP on the size of the surface micelles. The surface micelle diameter is found to increase with an increase in the bead number of R, which is consistent with the results observed in the experiments (Figure 2f).

The arrangement characteristics of these surface micelles were then analyzed (Figure 5f). Regarding the patterns formed by the R_6C_5 block copolymers, a sixfold coordination lattice is the dominant arrangement of the micelles. Fivefold and sevenfold coordinated surface micelle arrays are also observed, which are highlighted by red and green dots, respectively. The surface micelles formed by R_5C_5 and R_7C_5 possess similar array features. It is also noted that for all the three samples, there are more fivefold coordinated surface micelles than sevenfold coordinated surface micelles (see Table S4, Supporting Information). Similar to the experimental observations, the larger number of fivefold coordinated surface micelles can be attributed to the asymmetry in the size distribution of the surface micelles (see Figure S6, Supporting Information). From the size distribution, it is found that more than 50% of the surface micelles are smaller than the average size, which contributes to the fact that the number of fivefold coordinated surface micelles is greater than that of sevenfold coordinated ones. These theoretical simulation results are consistent with the experimental observations.

The construction of ordered surface nanostructures on substrates has attracted long-lasting interest. In most works, the formation of ordered surface nanostructures is devoted to the microphase-separation of block copolymer in thin films.[51] In addition to the thin film microphase separation of block copolymers, the interface self-assembly of block copolymers can be an alternative way to construct well-ordered surface nanostructures. In this work, we discovered that through the self-assembly of block copolymers at the selective solvent/substrate interface, the PBLG-*b*-PEG rod-coil block copolymers are capable of forming dot nanopatterns on a substrate. Different from the block copolymer thin films, the dot nanopatterns in our work are formed under the driving force of hydrophilic–hydrophobic balance of the block copolymers. It should be emphasized that since we know the factors that result in defects, i.e., the distribution of surface micelle size and irregular distribution of morphology, the defects can be regulated and eliminated by using more precisely defined block copolymers and optimizing the self-assembly procedures. In addition, applying external stimuli, for example, shear force[52] on the interface self-assembly of block copolymer could be beneficial to guide the arrangement of surface micelles, which could be a direction of future work.

3. Conclusions

In summary, we found in this work that PBLG-*b*-PEG rod-coil block copolymers can self-assemble on a planar substrate into surface micelles forming ordered dot nanopatterns. The experimental observations are well supported by theoretical simulations. For the surface micelles, the PBLG block forms the core and the PEG block forms the shell, and their diameter increases as the DP value of the PBLG block increases. An analysis of the surface micelle array characteristics shows that the majority of surface micelles are arranged in a sixfold coordination lattice. Due to the nonuniform size of the surface micelles and the existence of nonspherical surface micelles, defects such as fivefold coordination and sevenfold coordination lattices of the micelles are observed. This work provides a facile way to build ordered nanopatterns on substrates through an adsorption-assembly of block copolymers on planar substrates. The gained information could guide the design and preparation of materials with sophisticated patterns.

4. Experimental Section

Polymer Synthesis: PBLG-*b*-PEG block copolymers were obtained via ring-opening polymerization of γ-benzyl-L-glutamate-*N*-carboxyanhydride (BLG-NCA) initiated by mPEG-NH_2 in 1,4-dioxane.[12,13] PS-*b*-PEG block copolymers were synthesized in anisole by atom transfer radical polymerization (ATRP) of styrene using mPEG-Br as initiator in the presence of *N,N,N′,N″,N‴*-pentamethyldiethylene triamine (PMDETA) and copper(I) bromide (CuBr).[53] Details of the polymer synthesis are provided in Section S1 of the Supporting Information.

Preparation of the PS Substrate: PS substrates were prepared by spin-coating PS solutions on Si wafers and then performing a subsequent heat treatment. First, PS solutions were spin-coated on Si wafers. Then, the coated Si wafers were heat-treated so that the PS could irreversibly adsorb on the Si substrates and be stable in solvents.[24,25] Finally, the heat-treated Si wafers were cooled to room temperature and washed with clean toluene three times. Preparation details of the PS substrate are provided in Section S2.1 of the Supporting Information.

Preparation of the Nanopattern: The preparation process is illustrated in Scheme 1. In the first step, to the solution of PBLG-*b*-PEG in tetrahydrofuran/*N,N′*-dimethylformamide (THF/DMF, 3/7 v/v), the PS

substrate was introduced and being immersed for 1 h. In the second step, the PS substrate was taken out from the PBLG-*b*-PEG solution and transferred into a vial containing fresh THF/DMF solvent (3/7 v/v). Then, water was gradually added into the vial, which induces an in situ self-assembly of the block copolymers into surface micelles on the substrate. Finally, the substrate was taken out from the solution and rinsed with water. After air-drying, a dot nanopattern composed of surface micelles that were formed by the PBLG-*b*-PEG block copolymers on the substrate was obtained. The initial concentration of the block copolymer was 0.2 g L^{-1}, and the experiment temperature was 20 °C. Details of the preparation of the nanopattern are provided in Section S2.3 of the Supporting Information.

Characterizations: The DP and molecular weight distributions (Đ) of the block copolymers were obtained from ^{1}H nuclear magnetic resonance (NMR, Avance 550, Bruker) measurements and gel permeation chromatography (GPC, PL 50 plus) tests. The morphologies of the surface nanopatterns were characterized by AFM (XE-100, Park Systems). The sizes of the surface micelles were obtained by collecting AFM images with more than 500 micelles and analyzing the images using professional software (XEI, Park Systems).

Simulation Methods: Dissipative particle dynamics (DPD) simulation was used to study the structure of the surface micelles.[49,50] In the DPD simulation, a volume of atoms was represented by a coarse-grained DPD bead. In the present simulations, according to the molecular information of PBLG-*b*-PEG, a coarse-grained RC model consisting of a rod (R) block and a flexible (C) block was constructed. The neighboring beads in the RC were connected via a harmonic spring force. The rigidity of the R blocks was realized by a cosine harmonic function. The substrate covered by a PS layer was mapped as a planar substrate (W) covered by a coarse-grained homopolymer layer. Detailed simulation information is available in Section S10 of the Supporting Information.

Supporting Information

Supporting Information is available from the Wiley Online Library or from the author.

Acknowledgements

B.S. and Z.X. contributed equally to this work. This work was supported by the National Natural Science Foundation of China (51833003, 51621002, 21975073, and 51573049).

Conflict of Interest

The authors declare no conflict of interest.

Keywords

dot nanostructures, rod-coil block copolymers, self-assembly, surface micelles, theoretical simulations

Received: August 3, 2020
Published online: August 17, 2020

[1] A. Verma, O. Uzun, Y. Hu, Y. Hu, H.-S. Han, N. Watson, S. Chen, D. J. Irvine, F. Stellacci, *Nat. Mater.* **2008**, *7*, 588.
[2] T. Chang, H. Huang, T. He, *Macromol. Rapid Commun.* **2016**, *37*, 161.
[3] L. Guo, Y. Ding, J. Han, N. Xu, X. Lu, Y. Cai, *Macromol. Rapid Commun.* **2015**, *36*, 1505.
[4] Y. Mai, A. Eisenberg, *Chem. Soc. Rev.* **2012**, *41*, 5969.
[5] C. Choi, M. Go, S. Y. Park, S. Kang, Y. Seo, J. Lee, J. K. Kim, *ACS Appl. Mater. Interfaces* **2019**, *11*, 44636.
[6] C. Yang, X. Ma, J. Lin, L. Wang, Y. Lu, L. Zhang, C. Cai, L. Gao, *Macromol. Rapid Commun.* **2018**, *39*, 1700701.
[7] X. Gu, I. Gunkel, A. Hexemer, T. P. Russell, *Colloid Polym. Sci.* **2014**, *292*, 1795.
[8] C. Sinturel, M. Vayer, M. Morris, M. A. Hillmyer, *Macromolecules* **2013**, *46*, 5399.
[9] Y. S. Oh, K. H. Lee, H. Kim, D. Y. Jeon, S. H. Ko, C. P. Grigoropoulos, H. J. Sung, *J. Phys. Chem. C* **2012**, *116*, 11728.
[10] K. Han, L. Heng, L. Jiang, *ACS Nano* **2016**, *10*, 11087.
[11] N. Benoot, P. Marcasuzaa, L. Pessoni, S. Chasvised, S. Reynaud, A. Bousquet, L. Billon, *Soft Matter* **2018**, *14*, 4874.
[12] C. Cai, J. Lin, X. Zhu, S. Gong, X.-S. Wang, L. Wang, *Macromolecules* **2016**, *49*, 15.
[13] C. Cai, Y. Li, J. Lin, L. Wang, S. Lin, X.-S. Wang, T. Jiang, *Angew. Chem., Int. Ed.* **2013**, *52*, 7732.
[14] C. Cai, J. Lin, T. Chen, X.-S. Wang, S. Lin, *Chem. Commun.* **2009**, 2709.
[15] Y. Han, C. Cai, J. Lin, S. Gong, W. Xu, R. Hu, *Macromol. Rapid Commun.* **2018**, *39*, 1800080.
[16] J. D. Hill, P. C. Millett, *Macromolecules* **2019**, *52*, 9495.
[17] J. Henzie, J. E. Barton, C. L. Stender, T. W. Odom, *Acc. Chem. Res.* **2006**, *39*, 249.
[18] E. A. Minich, A. P. Nowak, T. J. Deming, D. J. Pochan, *Polymer* **2004**, *45*, 1951.
[19] Y. Liu, J. Goebl, Y. Yin, *Chem. Soc. Rev.* **2013**, *42*, 2610.
[20] S. Rath, M. Heilig, H. Port, J. Wrachtrup, *Nano Lett.* **2007**, *7*, 3845.
[21] W. D. Volkmuth, T. Duke, M. C. Wu, R. H. Austin, A. Szabo, *Phys. Rev. Lett.* **1994**, *72*, 2117.
[22] N. Stoop, J. Dunkel, *Soft Matter* **2018**, *14*, 2329.
[23] K. R. Gadelrab, Y. Ding, R. Pablo-Pedro, H. Chen, K. W. Gotrik, D. G. Tempel, C. A. Ross, A. Alexander-Katz, *Nano Lett.* **2018**, *18*, 3766.
[24] Y. Fujii, Z. Yang, J. Leach, H. Atarashi, K. Tanaka, O. K. C. Tsui, *Macromolecules* **2009**, *42*, 7418.
[25] C. Housmans, M. Sferrazza, S. Napolitano, *Macromolecules* **2014**, *47*, 3390.
[26] F. Xu, J. Zhang, P. Zhang, X. Luan, Y. Mai, *Mater. Chem. Front.* **2019**, *3*, 2283.
[27] V. M. De Cupere, J. F. Gohy, R. Jérome, P. G. Rouxhet, *J. Colloid Interface Sci.* **2004**, *271*, 60.
[28] S.-W. Kuo, C.-J. Chen, *Macromolecules* **2012**, *45*, 2442.
[29] S. Zhang, C. Cai, Q. Huang, J. Lin, Z. Xu, *Acta Polym. Sin.* **2018**, 109.
[30] A. M. Rosales, H. K. Murnen, S. R. Kline, R. N. Zuckermann, R. A. Segalman, *Soft Matter* **2012**, *8*, 3673.
[31] T. Abraham, S. Giasson, J. F. Gohy, R. Jérôme, B. Müller, M. Stamm, *Macromolecules* **2000**, *33*, 6051.
[32] H. D. Bijsterbosch, M. A. C. Stuart, G. J. Fleer, P. van Caeter, E. J. Goethals, *Macromolecules* **1998**, *31*, 7436.
[33] R. Toomey, J. Mays, J. Yang, M. Tirrell, *Macromolecules* **2006**, *39*, 2262.
[34] K. T. Kim, C. Park, G. W. M. Vandermeulen, D. A. Rider, C. Kim, M. A. Winnik, I. Manners, *Angew. Chem., Int. Ed.* **2005**, *44*, 7964.
[35] B. D. Olsen, R. A. Segalman, *Mater. Sci. Eng., R* **2008**, *62*, 37.
[36] M. Lee, B.-K. Cho, W.-C. Zin, *Chem. Rev.* **2001**, *101*, 3869.
[37] W. Xu, Z. Xu, C. Cai, J. Lin, S. Zhang, L. Zhang, S. Lin, Y. Yao, H. Qi, *J. Phys. Chem. Lett.* **2019**, *10*, 6375.
[38] X. Zhu, Z. Guan, J. Lin, C. Cai, *Sci. Rep.* **2016**, *6*, 29796.
[39] A. A. Abate, G. T. Vu, A. D. Pezzutti, N. A. García, R. L. Davis, F. Schmid, R. A. Register, D. A. Vega, *Macromolecules* **2016**, *49*, 7588.
[40] W. Li, M. Müller, *Annu. Rev. Chem. Biomol. Eng.* **2015**, *6*, 187.

[41] D. A. Vega, C. K. Harrison, D. E. Angelescu, M. L. Trawick, D. A. Huse, P. M. Chaikin, R. A. Register, *Phys. Rev. E* **2005**, *71*, 061803.
[42] K. Aissou, T. Baron, M. Kogelschatz, A. Pascale, *Macromolecules* **2007**, *40*, 5054.
[43] N. A. García, A. D. Pezzutti, R. A. Register, D. A. Vega, L. R. Gómez, *Soft Matter* **2015**, *11*, 898.
[44] N. A. Lynd, A. J. Meuler, M. A. Hillmyer, *Prog. Polym. Sci.* **2008**, *33*, 875.
[45] J. Zhang, X.-F. Chen, H.-B. Wei, X.-H. Wan, *Chem. Soc. Rev.* **2013**, *42*, 9127.
[46] A. Eberl, B. Klar, *Comput. Stat. Data An.* **2020**,*146*, 106939.
[47] M. R. Hammond, S. W. Sides, G. H. Fredrickson, E. J. Kramer, J. Ruokolainen, S. F. Hahn, *Macromolecules* **2003**, *36*, 8712.
[48] M. Kachanov, *Int. J. Fract.* **1999**, *97*, 1.
[49] Q. Zhang, J. Lin, L. Wang, Z. Xu, *Prog. Polym. Sci.* **2017**, *75*, 1.
[50] Z. Zhuang, T. Jiang, J. Lin, L. Gao, C. Yang, L. Wang, C. Cai, *Angew. Chem., Int. Ed.* **2016**, *55*, 12522.
[51] I. W. Hamley, *Nanotechnology* **2003**, *14*, R39.
[52] D. E. Angelescu, J. H. Waller, R. A. Register, P. M. Chaikin, *Adv. Mater.* **2005**, *17*, 1878.
[53] K. Matyjaszewski, J. Xia, *Chem. Rev.* **2001**, *101*, 2921.